

1    **Supplementary Information**

2    **pH affects the aqueous-phase nitrate-mediated photooxidation of phenolic compounds:**  
3    **Implications for brown carbon formation and evolution**

4    Junwei Yang,<sup>a</sup> Wing Chi Au,<sup>a</sup> Haymann Law,<sup>a</sup> Chun Hei Leung,<sup>a</sup> Chun Ho Lam,<sup>a</sup> Theodora  
5    Nah<sup>\*a</sup>

6    <sup>a</sup>*School of Energy and Environment, City University of Hong Kong, Hong Kong, China SAR*

7  
8    \* *To whom correspondence should be addressed: Theodora Nah (Email: theodora.nah@cityu.edu.hk, Tel: +852  
9    3442 5578, Postal address: School of Energy and Environment, Yeung Kin Man Academic Building, City  
10   University of Hong Kong, Tat Chee Avenue, Kowloon, Hong Kong)*

11

12

13

14

15

16

17

18

19

20

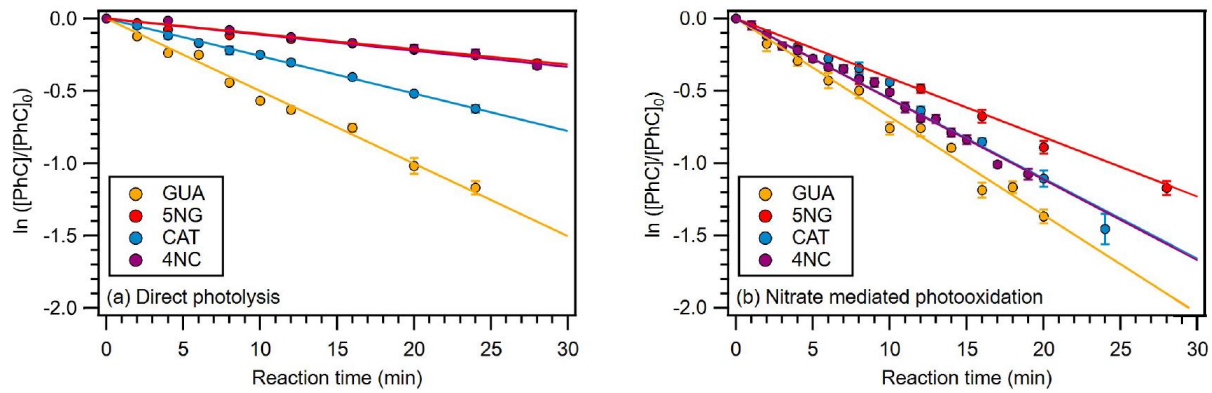
21

22

23

24

25



26

27 **Figure S1:** Kinetic decay results of the four phenolic compounds in (a) direct photolysis, and  
 28 (b) nitrate-mediated photooxidation experiments. Lines show the exponential fit to the kinetic  
 29 data. Error bars indicate standard deviations between multiple experiments.

30

31

32

33

34

35

36

37

38

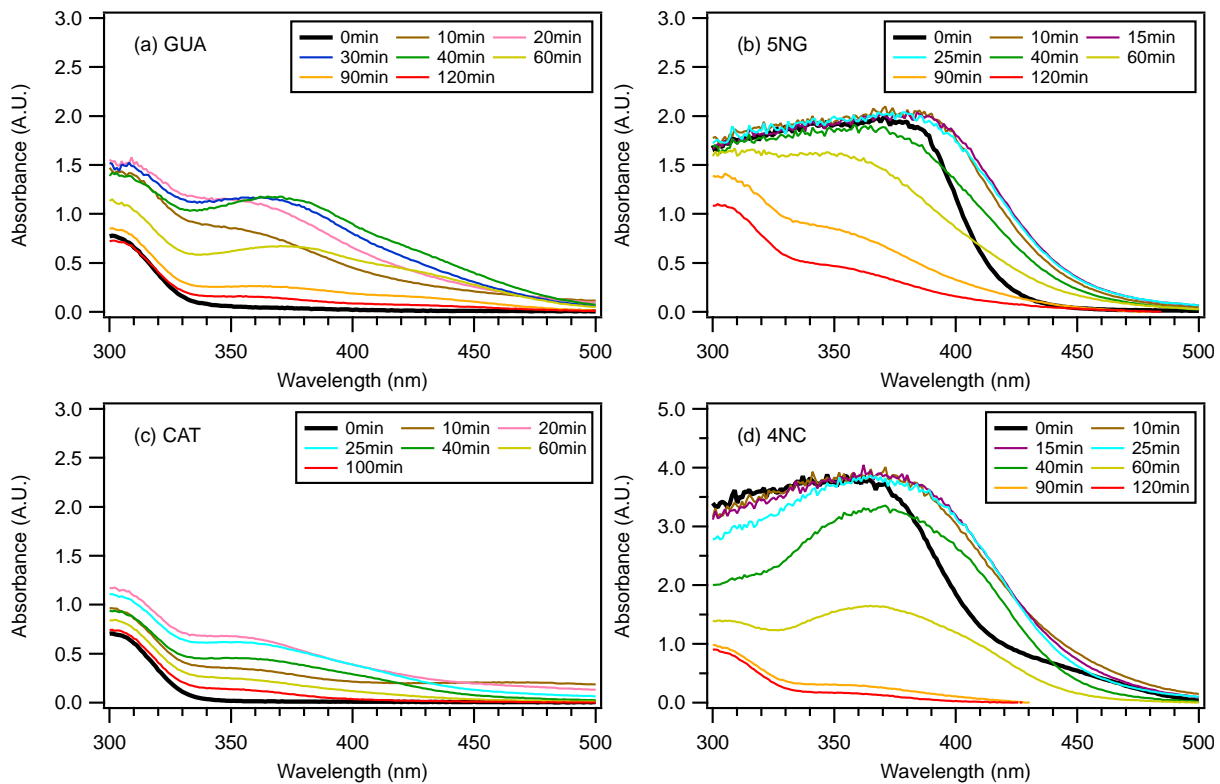


**Figure S2:** Absorption spectra of (a) guaiacol, (b) 5-nitroguaiacol, (c) catechol, and (d) 4-nitrocatechol during nitrate-mediated photooxidation at solution pH 6. These absorption spectra were taken at sequential time steps during the reaction.

39

40 **Figure S2:** Absorption spectra of (a) guaiacol, (b) 5-nitroguaiacol, (c) catechol, and (d) 4-  
41 nitrocatechol during nitrate-mediated photooxidation at solution pH 6. These absorption  
42 spectra were taken at sequential time steps during the reaction.

43

44

45

46

47

48

49

50

51

52

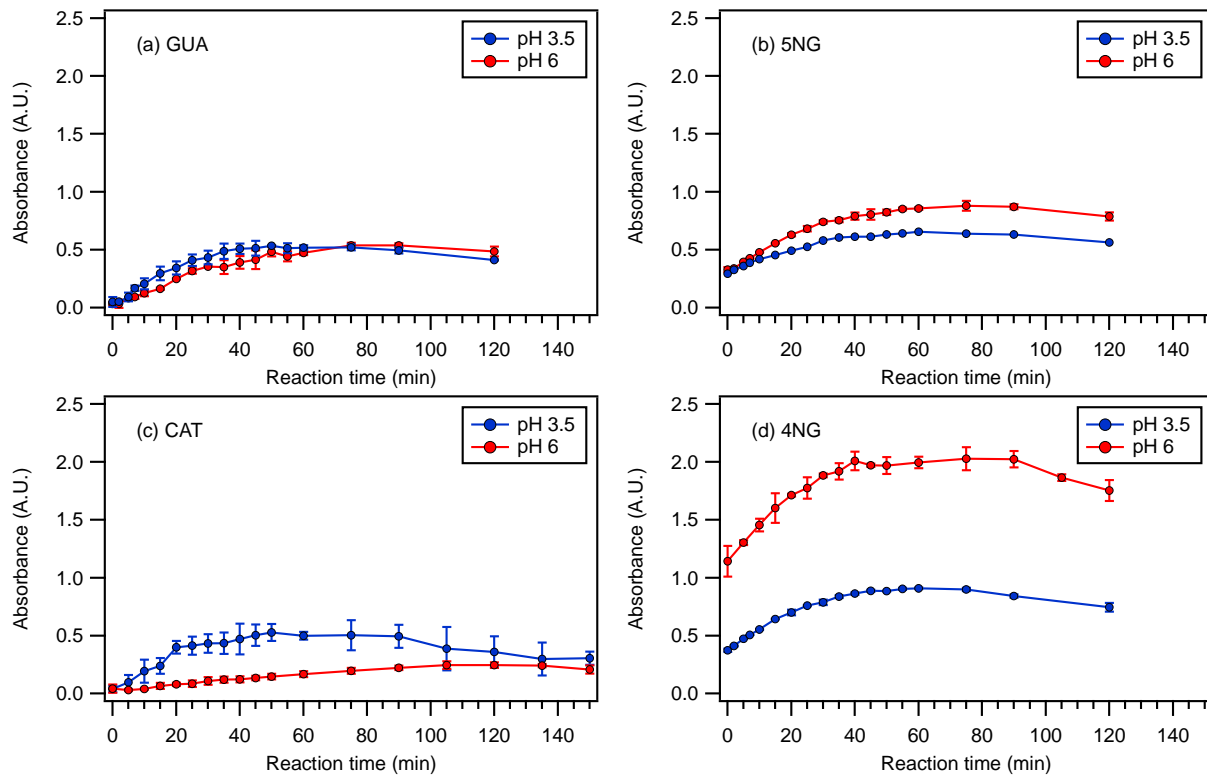


**Figure S3:** Changes in the absorbance of (a) guaiacol at 365 nm, (b) 5-nitroguaiacol and 420 nm, (c) catechol at 365 nm, and (d) 4-nitrocatechol at 420 nm during direct photolysis. The experiments were performed using solutions that were either unacidified (pH 6, red symbols and lines), or were acidified to pH 3.5 (blue symbols and lines). Error bars indicate standard deviations between multiple experiments.

53

54 **Figure S3:** Changes in the absorbance of (a) guaiacol at 365 nm, (b) 5-nitroguaiacol and 420  
 55 nm, (c) catechol at 365 nm, and (d) 4-nitrocatechol at 420 nm during direct photolysis. The  
 56 experiments were performed using solutions that were either unacidified (pH 6, red symbols  
 57 and lines), or were acidified to pH 3.5 (blue symbols and lines). Error bars indicate standard  
 58 deviations between multiple experiments.

59

60

61

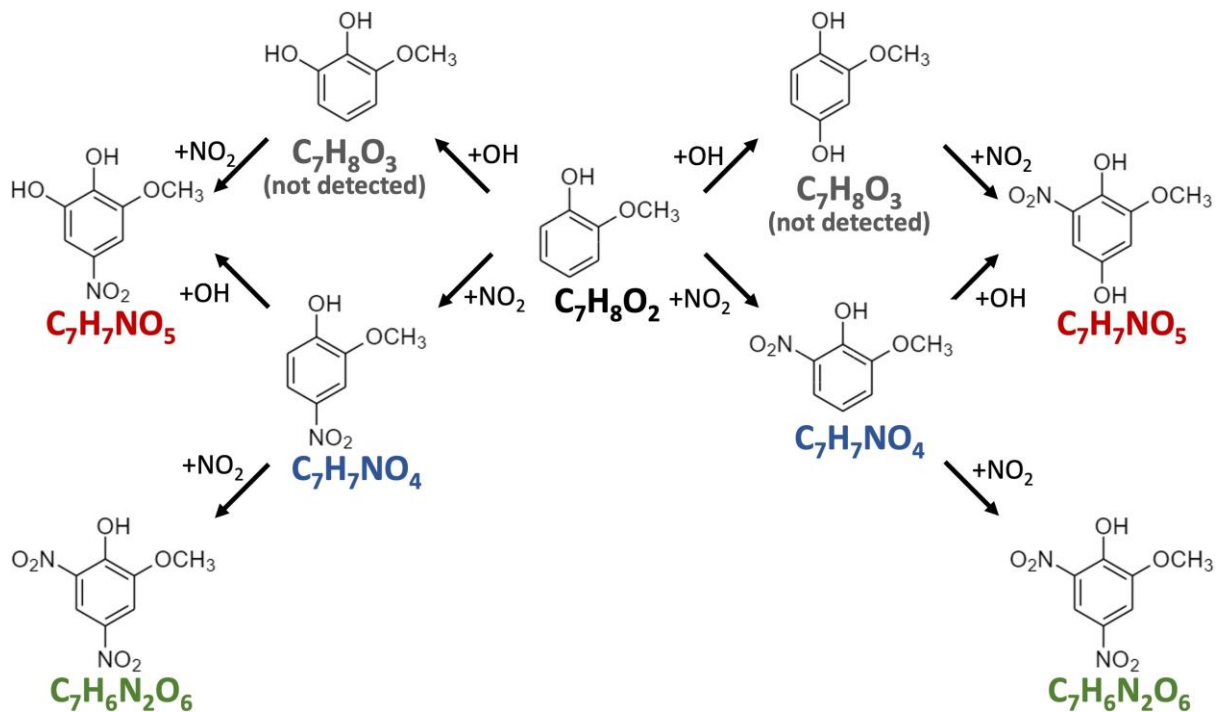
62

63

64

65

66

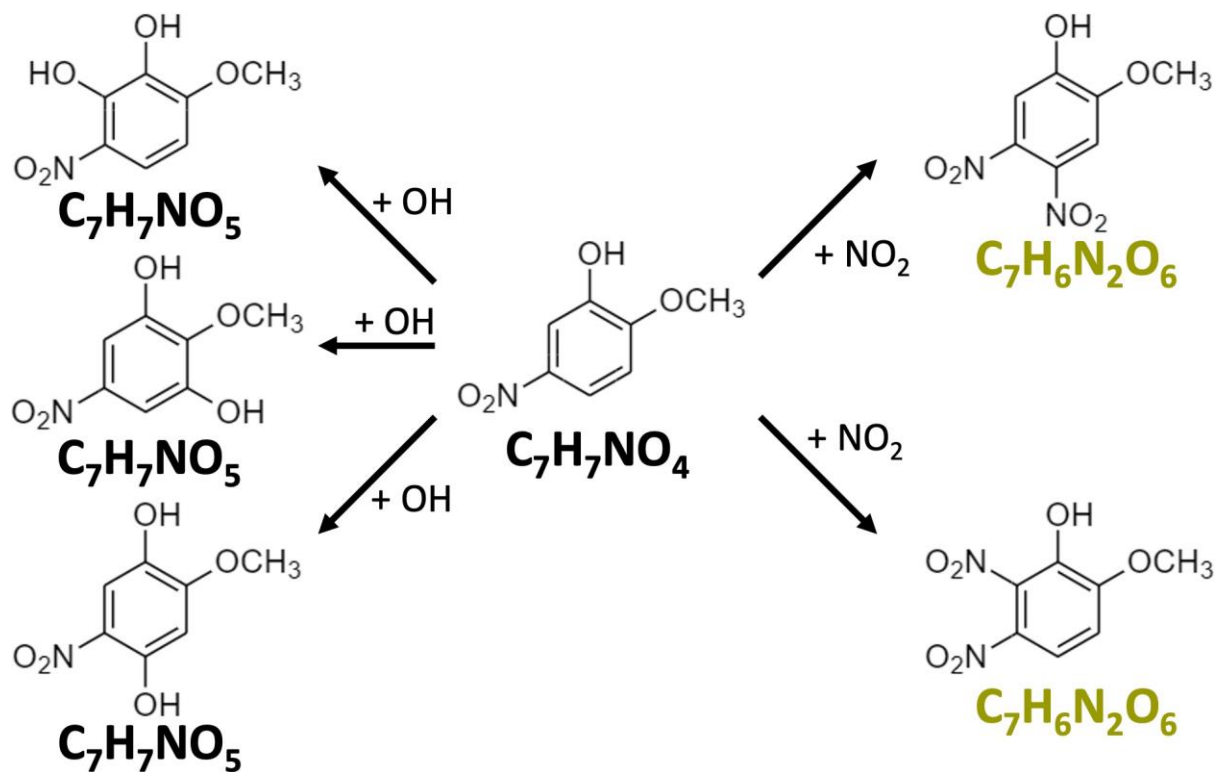


67 **Figure S4:** Proposed structures of the prominent products measured by the UPLC-MS during  
68 the nitrate-mediated photooxidation of guaiacol. Note that although this figure proposes that  
69 several isomers can potentially be formed for some of these products, only one isomer is  
70 detected most of the time, and MS/MS analysis is usually unable to conclusively determine the  
71 chemical structures of the detected isomer. All the products will undergo further reaction, which  
72 will eventually lead to ring-opening and the formation of smaller, highly oxygenated molecules.  
73 Note that while  $C_7H_8O_3$  can be a potential first-generation product, it was not detected.

74  
75

76

77



78

79 **Fig. S5:** Proposed structures of the prominent products measured by the UPLC-MS during the  
80 nitrate-mediated photooxidation of 5-nitroguaiacol. Note that although this figure proposes that  
81 several isomers can potentially be formed for some of these products, only one isomer is  
82 detected most of the time, and MS/MS analysis is usually unable to conclusively determine the  
83 chemical structures of the detected isomer. All the products will undergo further reaction, which  
84 will eventually lead to ring-opening and the formation of smaller, highly oxygenated molecules.

85

86

87

88

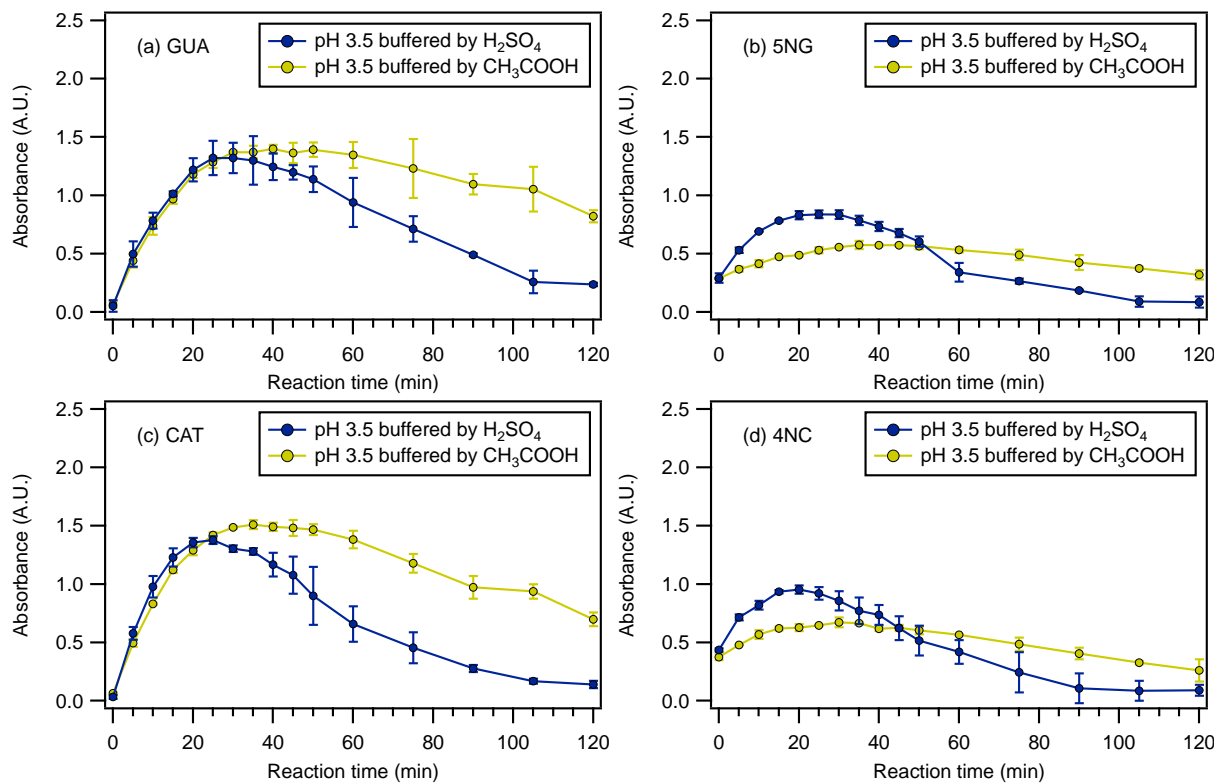
89

90

91

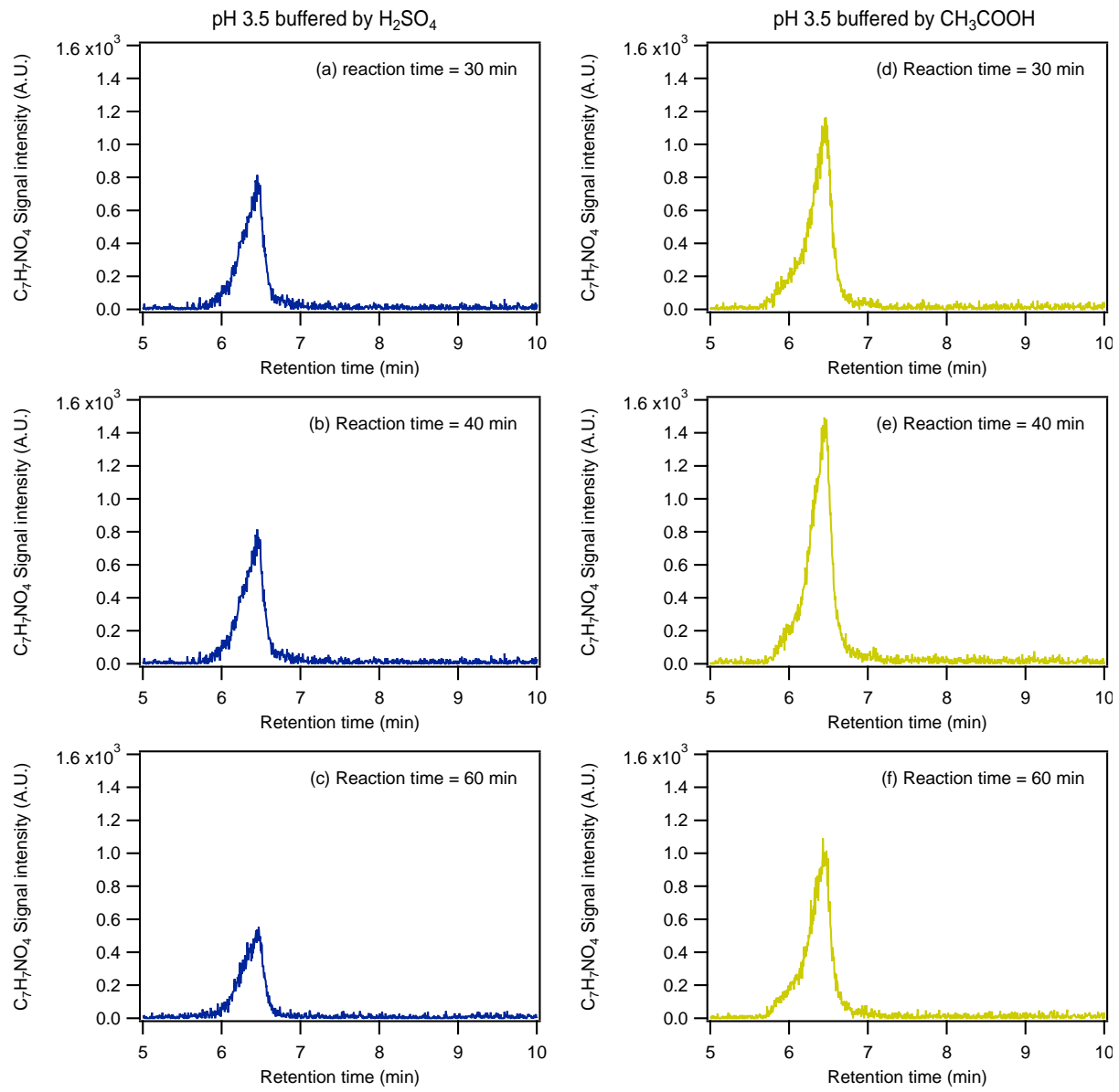
92

93

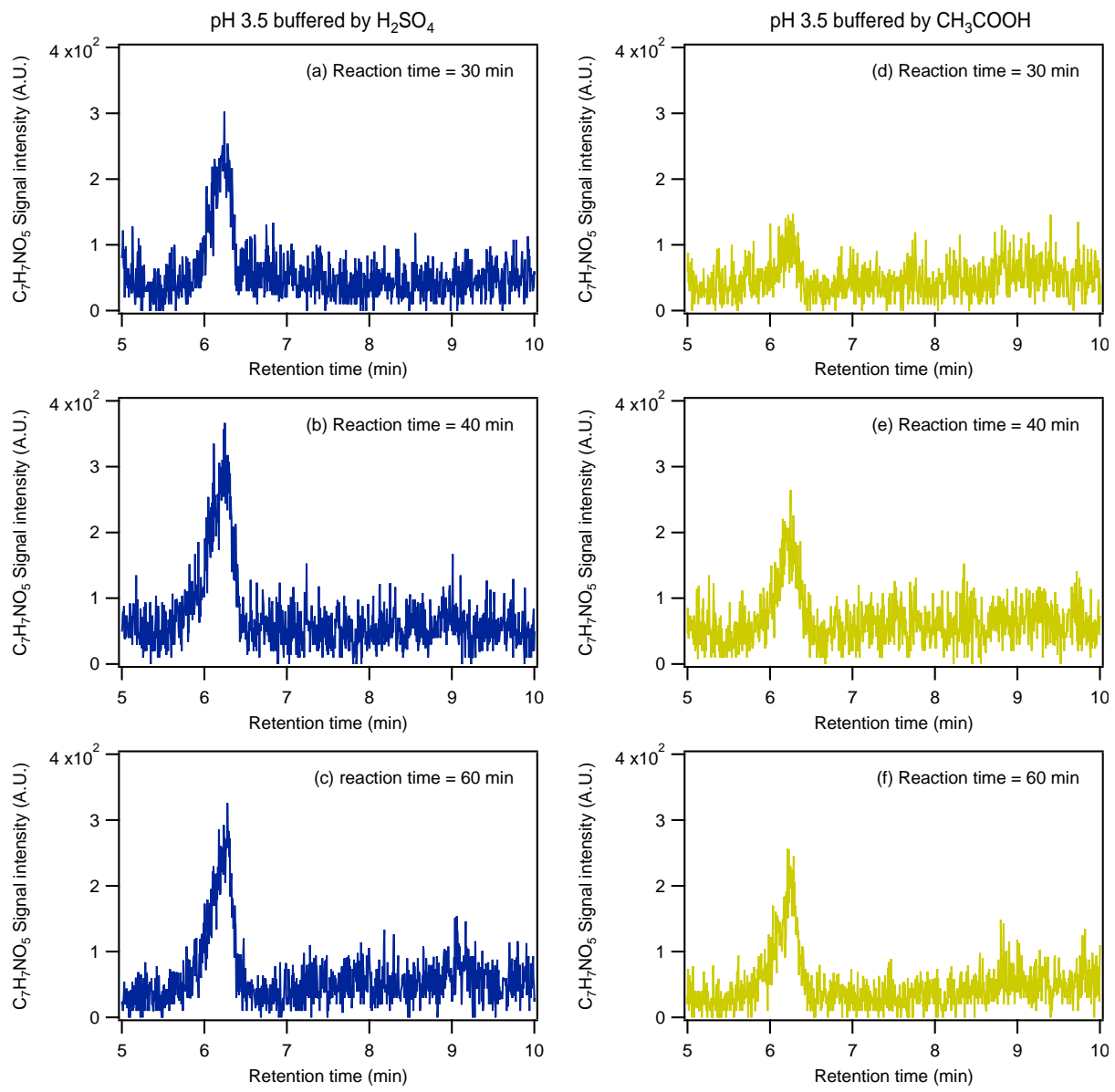


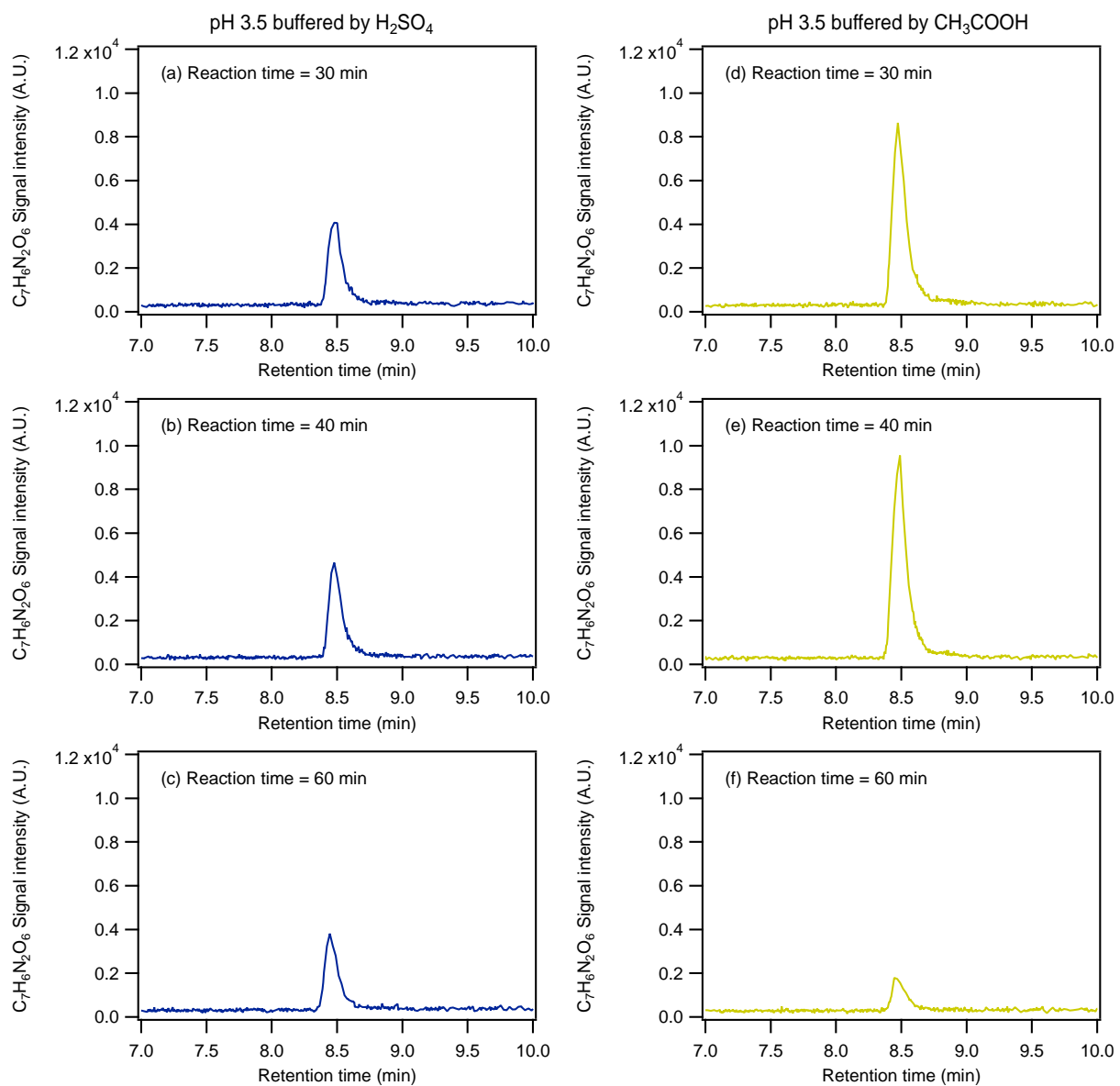
94

95 **Figure S6:** Changes in the absorbance of (a) guaiacol at 365 nm, (b) 5-nitroguaiacol at 420 nm,  
96 (c) catechol at 365 nm, and (d) 4-nitrocatechol at 420 nm during nitrate-mediated  
97 photooxidation. The experiments were performed using solutions that were either acidified  
98 with  $\text{H}_2\text{SO}_4$  (blue symbols and lines) or with  $\text{CH}_3\text{COOH}$  (green symbols and lines). Error bars  
99 indicate standard deviations between multiple experiments.



100  
101 **Figure S7:** XIC chromatograms of  $\text{C}_7\text{H}_7\text{NO}_4$  during the nitrate-mediated photooxidation of  
102 guaiacol at  $\text{pH } 3.5$  using  $\text{CH}_3\text{COOH}$ -acidified (right side) vs.  $\text{H}_2\text{SO}_4$ -acidified (left side)  
103 solutions at reaction times 30 min, 40 min, and 60 min.





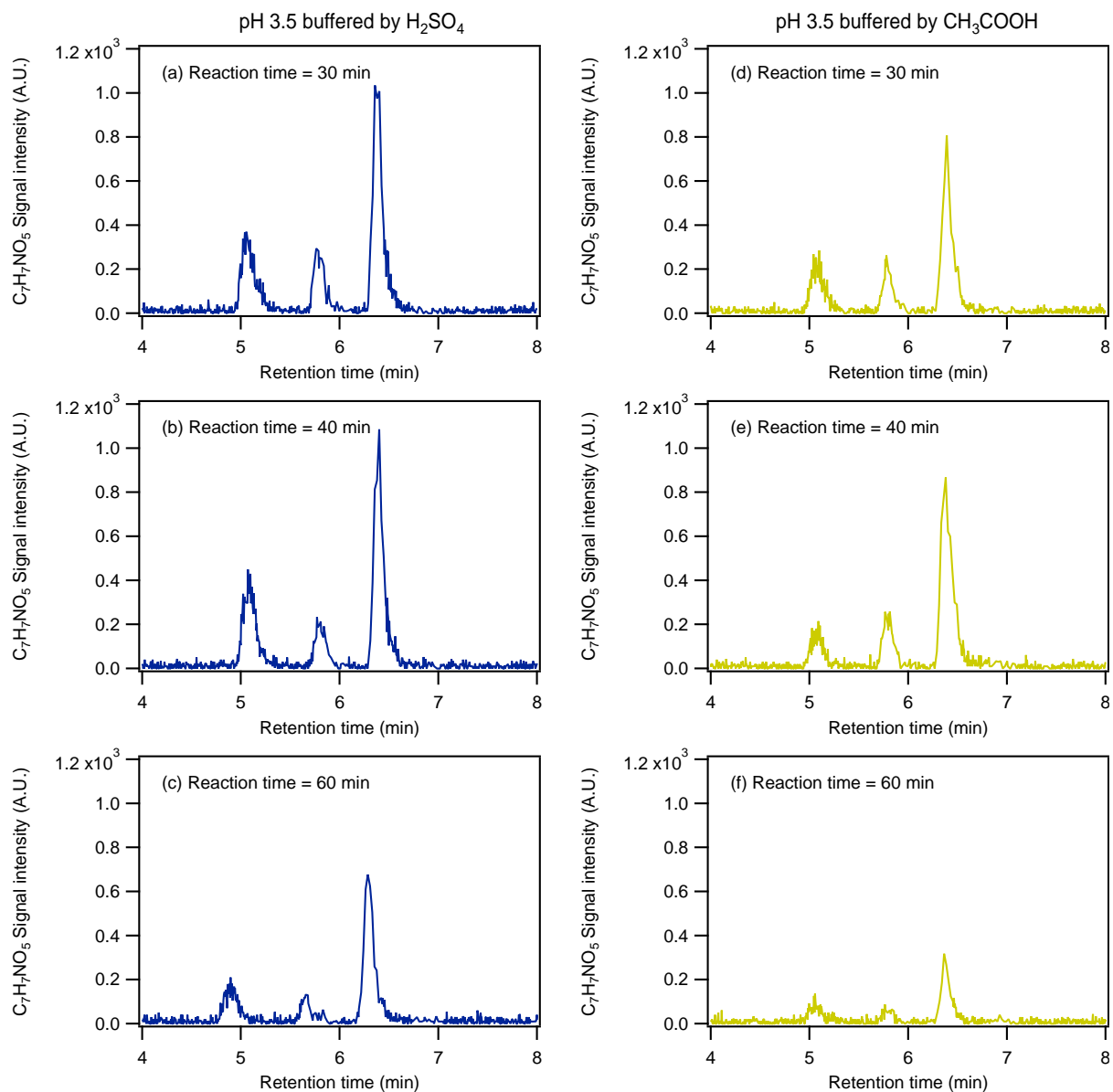


**Figure S10:** XIC chromatograms of  $C_7H_7NO_5$  isomers during the nitrate-mediated photooxidation of 5-nitroguaiacol at pH 3.5 using  $CH_3COOH$ -acidified (right side) vs.  $H_2SO_4$ -acidified (left side) solutions at reaction times 30 min, 40 min, and 60 min.

112

113

114

115

116

117

118

119

120

121

122 **Table S1.** The photoreaction pathways initiated by the aqueous-phase photolysis of inorganic  
 123 nitrate.<sup>1-3</sup>

No.	Reactions	Quantum yield ( $\Phi$ )/ Acid dissociation constant (pK <sub>a</sub> )
1	$\text{NO}_3^- + \text{h}\nu \rightarrow [\bullet\text{NO}_2 + \text{O}\bullet^-]_{\text{cage}}$	$\Phi = 0.01$
2	$[\bullet\text{NO}_2 + \text{O}\bullet^-]_{\text{cage}} \rightarrow \bullet\text{NO}_2 + \text{O}\bullet^-$	—
3	$\text{O}\bullet^- + \text{H}_2\text{O} \rightleftharpoons \bullet\text{OH} + \text{OH}^-$	$\text{pK}_a(\bullet\text{OH}) = 11.9$
4	$[\bullet\text{NO}_2 + \text{O}\bullet^-]_{\text{cage}} \rightarrow \text{OONO}^-$	—
5	$\text{OONO}^- + \text{H}^+ \rightleftharpoons \text{HOONO}$	$\text{pK}_a = 7$
6	$\text{HOONO} \rightarrow \bullet\text{OH} + \bullet\text{NO}_2$	—
7	$2 \bullet\text{NO}_2 \rightleftharpoons \text{N}_2\text{O}_4$	—
8	$\text{N}_2\text{O}_4 + \text{H}_2\text{O} \rightarrow \text{HNO}_2 + \text{NO}_3^- + \text{H}^+$	—
9	$\text{HNO}_2 \rightleftharpoons \text{H}^+ + \text{NO}_2^-$	$\text{pK}_a = 3 \sim 3.5$
10	$\text{NO}_2^- + \text{h}\nu \rightarrow \bullet\text{NO} + \text{O}\bullet^-$	$\Phi = 0.025\text{--}0.065$
11	$\text{NO}_2^- + \text{h}\nu \rightarrow \bullet\text{NO}_2 + \text{e}^-$	$\Phi = \sim 0.001$
12	$\text{NO}_2^- + \bullet\text{OH} \rightarrow \bullet\text{NO}_2 + \text{OH}^-$	—
13	$\bullet\text{NO} + \bullet\text{NO}_2 \rightleftharpoons \text{N}_2\text{O}_3$	—
14	$\text{N}_2\text{O}_3 + \text{H}_2\text{O} \rightarrow 2 \text{NO}_2^- + 2 \text{H}^+$	—
15	$\text{HNO}_2 + \text{h}\nu \rightarrow \bullet\text{NO} + \bullet\text{OH}$	$\Phi = 0.35$
16	$\text{HNO}_2 + \bullet\text{OH} \rightarrow \bullet\text{NO}_2 + \text{H}_2\text{O}$	—
17	$2 \text{HNO}_2 \rightarrow \bullet\text{NO} + \bullet\text{NO}_2 + \text{H}_2\text{O}$	—

124

125

126

127

128

129

130 **Table S2.** Experimental conditions for the aqueous-phase nitrate-mediated photooxidation of  
 131 guaiacol, catechol, 5-nitroguaiacol, and 4-nitrocatechol.

Experiment	Phenolic compounds	pH	NH <sub>4</sub> NO <sub>3</sub> (μM)	Acid added
1	2 μM guaiacol	6	200	—
2	2 μM guaiacol	3.5	200	H <sub>2</sub> SO <sub>4</sub>
3	2 μM guaiacol	3.5	200	CH <sub>3</sub> COOH
4	2 μM 5-nitroguaiacol	6	200	—
5	2 μM 5-nitroguaiacol	3.5	200	H <sub>2</sub> SO <sub>4</sub>
6	2 μM 5-nitroguaiacol	3.5	200	CH <sub>3</sub> COOH
7	2 μM catechol	6	200	—
8	2 μM catechol	3.5	200	H <sub>2</sub> SO <sub>4</sub>
9	2 μM catechol	3.5	200	CH <sub>3</sub> COOH
10	2 μM 4-nitrocatechol	6	200	—
11	2 μM 4-nitrocatechol	3.5	200	H <sub>2</sub> SO <sub>4</sub>
12	2 μM 4-nitrocatechol	3.5	200	CH <sub>3</sub> COOH

132

133

134

135

136

137

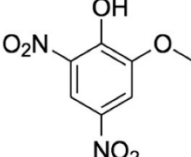
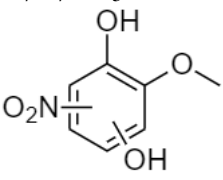
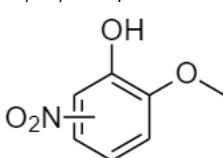
138

139

140

141

142 **Table S3:** List of products detected during the nitrate-mediated photooxidation of guaiacol at  
 143 pH 6 and pH 3.5 identified using UPLC-MS.

No.	Retention time (min)	m/z	Proposed product molecular formula and structure	MS/MS fragments
1	2.29	186.1128	$C_{11}H_{13}N_3$	Unknown
2	2.34	172.0973	$C_{10}H_{11}N_3$	Unknown
3	5.95	213.0146	$C_7H_6N_2O_6$ 	—CH <sub>3</sub> —NO <sub>2</sub>
4*	6.23	184.0258	$C_7H_7NO_5$ 	—OH —CH <sub>3</sub>
5*	6.41	168.0295	$C_7H_7NO_4$ 	—NO <sub>2</sub> —CH <sub>3</sub>
6	7.96	323.2333	Unknown	Unknown
7	11.50	157.1230	$C_9H_{18}O_2$	Unknown

144 \* Only these two products were detected in pH 3.5.

145

146

147

148

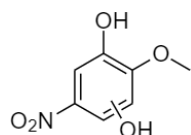
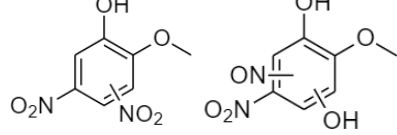
149

150

151

152

153 **Table S4:** List of products detected during the nitrate-mediated photooxidation of 5-  
 154 nitroguaiacol at pH 6 and pH 3.5 identified using UPLC-MS.

No.	Retention time (min)	m/z	Proposed product molecular formula and structure	MS/MS fragments
1*	5.07	184.0258	$C_7H_7NO_5$	Unknown
2**	5.17	172.0248	$C_6H_7NO_5$	Unknown
3*	5.69	139.0035	Unknown	Unknown
4**	5.80	184.0258	$C_7H_7NO_5$	Unknown
5**	6.40	184.0258	$C_7H_7NO_5$ 	—OH —CH <sub>3</sub>
6	7.74	224.0282	Unknown	Unknown
7**	8.47	213.0141	$C_7H_6N_2O_6$ 	—CH <sub>3</sub>
8	9.23	224.0306	$C_8H_7N_3O_5$	Unknown
9	9.28	223.0285	Unknown	Unknown

\* These two products were only detected at pH 3.5.

\*\* These four products were detected at both pH 6 and pH 3.5.

155  
156  
157

158

159

160

161

162

163

164

165

166 **S1. Determination of the steady-state OH radical concentrations in photooxidation**  
167 **experiments initiated by NH<sub>4</sub>NO<sub>3</sub> photolysis**

168 The steady-state OH radical concentrations ( $[\text{OH}]_{\text{ss}}$ ) in nitrate-mediated photooxidation  
169 experiments were measured separately using the method described in our previous work.<sup>4</sup>  
170 Benzoic acid (99.5%, J&K Scientific) was used as the probe compound to estimate the  $[\text{OH}]_{\text{ss}}$ .  
171 Similar concentrations (i.e., 2  $\mu\text{M}$  benzoic acid and 200  $\mu\text{M}$  NH<sub>4</sub>NO<sub>3</sub>) and reaction conditions  
172 were used in these separate experiments. Briefly, the time-dependent formation of 4-  
173 hydroxybenzoic acid was measured in these experiments. 4-hydroxybenzoic acid was assumed  
174 to be produced only from the OH + benzoic acid reaction with a yield of 0.17.<sup>5</sup> The time-  
175 dependent concentrations of benzoic acid that reacted with OH radicals was then determined  
176 from the time-dependent formation of 4-hydroxybenzoic acid.  $[\text{OH}]_{\text{ss}}$  was calculated using the  
177 time-dependent concentrations of benzoic acid which reacted with OH radicals and the second-  
178 order reaction rate constant for the OH + benzoic acid reaction ( $5.9 \times 10^9 \text{ M}^{-1} \text{ s}^{-1}$ ).<sup>6</sup> The  
179 measured  $[\text{OH}]_{\text{ss}}$  concentrations were within the range of [OH] values in atmospheric  
180 cloudwater ( $10^{-16}$  to  $10^{-12} \text{ M}$ ).<sup>7</sup>

181 4-hydroxybenzoic acid in separate  $[\text{OH}]_{\text{ss}}$  quantification experiments was measured  
182 using an ultra-high performance liquid chromatography system (1290 Infinity LC, Agilent)  
183 coupled to a high-resolution quadrupole-time-of-flight mass spectrometer (Sciex X500R  
184 QTOF) equipped with an ESI source that was operated in negative mode. All the samples were  
185 desalted using the SPE procedure described above. A reverse phase Kinetex (Phenomenex) PS-  
186 C18 column (150  $\times$  2.1 mm, 2.6  $\mu\text{m}$ , 100  $\text{\AA}$ ) equipped with a security guard and a PS-C18 pre-  
187 column was used for UPLC-MS analysis. The temperatures for the column oven and the UPLC  
188 autosampler were set to 25 °C. A gradient elution program was used. The binary mobile phases  
189 consisted of A (10 mM ammonium acetate) and B (acetonitrile) delivered at a flow rate 300  $\mu\text{L}$   
190  $\text{min}^{-1}$ . The sample injection volume was set to 10  $\mu\text{L}$ . The following mobile phase gradient  
191 was used: 0 to 3 min 1% B, 3 to 5 min linear gradient to 80% B, 5 to 6 min 80% B, 6 to 6.5  
192 min linear gradient to 1% B, 6.5 to 7 min 1% B. The following tandem MS conditions were  
193 used: -4500 V ESI ion spray voltage, -80 V declustering potential, -15 V collision energy, 25  
194 PSI curtain gas, and 450 °C source temperature.

195 **S2. Sample pretreatment by solid phase extraction (SPE)**

196 SPE was performed on all the samples using SPE cartridges (HLB, 60 mg, 3 cc, 30  $\mu$ m,  
197 Waters) to desalt the samples before UPLC-MS analysis. The SPE procedure used was as  
198 follows: Firstly, the SPE cartridge was activated and conditioned by filling it with 1 mL  
199 methanol and 1 mL ultrapure water. After that, 3 mL sample solution was loaded to the SPE  
200 cartridge. Then, the cartridge was flushed by adding 10 mL ultrapure water and dried by  
201 flushing air through the cartridge using an air pump. Finally, the elution was conducted by the  
202 addition of 3 mL acetonitrile and dried with flushing air. The eluted acetonitrile with organic  
203 compounds was collected for UPLC-MS analysis.

204

205 **References**

- 206 1. J. Mack and J. R. Bolton, Photochemistry of nitrite and nitrate in aqueous solution: A  
207 review, *Journal of Photochemistry and Photobiology A: Chemistry*, 1999, **128**, 1-13.
- 208 2. G. Marussi and D. Vione, Secondary Formation of Aromatic Nitroderivatives of  
209 Environmental Concern: Photonitration Processes Triggered by the Photolysis of  
210 Nitrate and Nitrite Ions in Aqueous Solution, *Molecules*, 2021, **26**, 2550.
- 211 3. D. Vione, B. Sur, B. K. Dutta, V. Maurino and C. Minero, On the effect of 2-propanol  
212 on phenol photonitration upon nitrate photolysis, *Journal of Photochemistry and*  
*Photobiology A: Chemistry*, 2011, **224**, 68-70.
- 213 4. J. Yang, W. C. Au, H. Law, C. H. Lam and T. Nah, Formation and evolution of brown  
214 carbon during aqueous-phase nitrate-mediated photooxidation of guaiacol and 5-  
215 nitroguaiacol, *Atmospheric Environment*, 2021, **254**, 118401.
- 216 5. C. Anastasio and K. G. McGregor, Chemistry of fog waters in California's Central  
217 Valley: 1. In situ photoformation of hydroxyl radical and singlet molecular oxygen,  
*Atmospheric Environment*, 2001, **35**, 1079-1089.
- 218 6. H. Herrmann, D. Hoffmann, T. Schaefer, P. Bräuer and A. Tilgner, Tropospheric  
219 aqueous-phase free-radical chemistry: radical sources, spectra, reaction kinetics and  
220 prediction tools, *Chemphyschem*, 2010, **11**, 3796-3822.
- 221 7. H. Herrmann, T. Schaefer, A. Tilgner, S. A. Styler, C. Weller, M. Teich and T. Otto,  
222 Tropospheric Aqueous-Phase Chemistry: Kinetics, Mechanisms, and Its Coupling to a  
223 Changing Gas Phase, *Chemical Reviews*, 2015, **115**, 4259-4334.

226